DNA in Nanopores: Counterion Condensation and Coion Depletion

Yitzhak Rabin[1] and Motohiko Tanaka[2]

[1]*Institute for Mathematics and Its Applications, University of Minnesota, Minneapolis, Minnesota 55255, USA and Department of Physics, Bar-Ilan University, Ramat-Gan 52900, Israel*

[2]*National Institute for Fusion Science, Toki 509-5292, Japan*

(Received 8 December 2004; published 15 April 2005)

Molecular dynamics simulations are used to study the equilibrium distribution of monovalent ions in a nanopore connecting two water reservoirs separated by a membrane, both for the empty pore and that with a single stranded DNA molecule inside. In the presence of DNA, the counterions condense on the stretched macromolecule effectively neutralizing it, and nearly complete depletion of coions from the pore is observed. The implications of our results for experiments on DNA translocation through α-hemolysin nanopores are discussed.

DOI: 10.1103/PhysRevLett.94.148103 PACS numbers: 87.15.Aa, 87.15.Ya, 87.14.Gg

Recent experiments on translocation of a single stranded (ss) DNA molecule through an α-hemolysin nanopore inserted in a membrane [1–5] have prompted a number of theoretical studies [6,7]. These studies, as well as other models of polymer translocation through narrow pores [8–15], focused on the polymer aspects of the problem such as the effect of confinement-induced entropy losses on the translocation of a Gaussian chain and on the effective friction between the chain and the narrow pore. The fact that DNA is a charged object was considered only as far as the mechanism of pulling by an externally applied potential gradient was concerned. While the above theories were quite successful in reproducing the observed distribution of translocation times [6] and the molecular weight dependence of the translocation velocity [7], some important questions remain unanswered. For example, as has been noted in Ref. [6], the theory overestimates (by more than an order of magnitude) the effective pulling force on the DNA. A similar discrepancy concerning the magnitude of the force acting on DNA, which suggests that its effective charge in the nanopore may be an order of magnitude smaller than the bulk solution value, has been observed in recent experiments on nanopore-induced opening of DNA hairpins [16,17]. Furthermore, while the models focus on the kinetics of DNA translocation through the pore, experiments probe this process only indirectly, by monitoring the transient blocking of the current of small ions through the channel. It is therefore essential to understand the physics of these ions in confined space—their interactions with the pore and with the DNA molecule, as well as their mutual interactions. Notice that even though the inner diameter of the α-hemolysin pore is much larger than the size of a small ion, the presence of negatively charged DNA is expected to have a dramatic effect on the distribution of small ions in the pore.

We proceed to study the problem by molecular dynamics simulations. We take an isolated rectangular box of three sides 56 Å, 56 Å, and 112 Å in the x, y, and z directions, respectively. This box is separated into upper and lower compartments by a membrane of thickness 50 Å. The center of the membrane is permeated by a cylindrical pore of radius 7.5 Å positioned along the z axis and assumed to be neutral (we do not account for the presence of charged and polar amino acids at the membrane-water interface [18]). In the absence of DNA, the simulation box is filled with three particle species, namely, counterions, coions, and water molecules that are free to move throughout the upper and lower compartments and through the pore, but cannot permeate the volume occupied by the membrane. The counterions and coions are spheres of radii 1.3 Å and 1.8 Å corresponding to ionic radii of K^+ and Cl^-, respectively, having either a positive or negative unit charge at their centers. There are 100 salt ions of each sign in the simulation box, corresponding to salt concentration of about 1 M. Water molecules are emulated by putting a sphere of radius 1.2 Å in every $(2.9\ \text{Å})^3$ volume, typically amounting to 6800 particles (a value smaller than the van der Waals radius of water was taken in order to speed up the simulation). The electrostatic properties of water and of the membrane have been taken into account by treating them as dielectric continua with $\varepsilon_w = 80$ and $\varepsilon_m = 2$, respectively, and matching the two dielectrics by introducing a 2.1 Å thick transition layer at the water-membrane boundary, across which the dielectric constant changes linearly from the former to the latter value. Reflecting boundary conditions are assumed at the surfaces of the rectangular box and of the membrane, and at the pore wall.

The ssDNA is modeled as a flexible chain of 12 repeat units, each of which contains a backbone made of a spherical bead with charge $-e$ at its center (phosphate group) connected to a noncharged bead (sugar ring), to which an additional noncharged bead (base) is attached. The beads are connected by effective springs and undergo thermal fluctuations under the constraint that the center of the macromolecule is pinned down at the pore center. The radii of the charged, noncharged, and side-chain beads

 © 2005 The American Physical Society

TABLE I. The average numbers (and variances) of counterions (N_+), coions (N_-), and of DNA charges (N_-^{DNA}) in a pore of 7.5 Å radius embedded in membranes of low ($\varepsilon_m = 2$) and high ($\varepsilon_m = 80$) dielectric constants are summarized. The net charge in the pore in units of electron charge (Q/e) and the end-to-end distance (R) of ssDNA within the pore are also shown. Only ions and DNA charges with centers further than 1.8 Å away from the ends of the pore were counted in order to minimize end effects.

	Empty ($\varepsilon_m = 2$)	ssDNA ($\varepsilon_m = 2$)	ssDNA ($\varepsilon_m = 80$)	Abasic DNA ($\varepsilon_m = 2$)
N_+	2.2 ± 1.5	11.5 ± 1.0	11.8 ± 1.2	12.3 ± 1.1
N_-	2.2 ± 1.6	0.4 ± 0.5	1.7 ± 0.9	0.9 ± 0.8
N_-^{DNA}	$\cdots$	11.7 ± 0.5	11.8 ± 0.4	12.0 ± 0.1
Q/e	0.06 ± 0.7	-0.6 ± 0.9	-1.7 ± 1.2	-0.6 ± 0.7
R	$\cdots$	44 Å	42 Å	35 Å

are taken as 2.1 Å, 1.8 Å, and 2.2 Å, respectively (the latter value corresponds to an adenine base). When DNA is present, 12 additional counterions are added to the system.

For each instantaneous spatial configuration of the charges, the electrostatic potential $\Phi(\mathbf{x})$ obeys the Poisson equation $\nabla \cdot (\epsilon \nabla \Phi) = -4\pi\rho$, where the charge density ρ is obtained by summation over ions $\rho(\mathbf{x}) = \sum_i q_i S(\mathbf{x} - \mathbf{x}_i)$, with S being a smeared $\delta-$ function (with the boundary condition $\Phi = 0$ on the surface of the box). This equation is solved numerically using the conjugate-gradient method with grid spacings 0.7 Å in the x, y directions and 1.1 Å in the z direction. The force on the ith particle is then given by $\mathbf{F}_i = -\nabla(q_i\Phi + U_{\mathrm{LJ}}) + \Delta(q_i \sum_j q_j \hat{\mathbf{r}}_{ij}/\epsilon r_{ij}^2)$, where the last term accounts for the short-range correction to the electrostatic force (the summation is taken over nearby ions within a Bjerrum length, 7 Å, and is computed in every time step). Since the rapid variation of the electrostatic force between neighboring charges is taken into account by this term, the remaining contribution to the electrostatic potential (Φ) is calculated by solving the Poisson equation only once in every 10 time steps. The volume exclusion of particle cores is incorporated through the Lennard-Jones potential $U_{\mathrm{LJ}}(\mathbf{r}_i) = \sum_j 4\epsilon_{\mathrm{LJ}}[(\sigma/r_{ij})^{12} - (\sigma/r_{ij})^6]$ for $r_{ij} \leq 2^{1/6}\sigma$ and $U_{\mathrm{LJ}} = -\epsilon_{\mathrm{LJ}}$ otherwise, where $\mathbf{r}_{ij} = \mathbf{r}_i - \mathbf{r}_j$ and σ is the sum of the radii of the two interacting particles. The temperature T is used as the energy scale and $\epsilon_{\mathrm{LJ}} = k_B T$ is assumed for simplicity.

We first consider a nanopore without DNA. We run the simulation for 4000 ps (our time step corresponds to 3.4 fs) and average the results over time. Inspection of Table I shows that on the average there are about 2.2 counterions and the same number of coions in the pore; however, the fluctuations are of the same magnitude as the average. This value is lower than that (4) corresponding to a uniform distribution of ions in the system, in agreement with the expectation that ions are repelled from the pore because the electrostatic self-energy of an ion in the pore is higher than in the bulk, due to the low dielectric constant of the surrounding membrane [19]. In order to clarify the underlying physics, in Fig. 1(a) we plot time histograms of the numbers of counterions (N_+), coions (N_-), and the total charge (Q) in the pore. Notice that even though the fluctuations around the mean values are quite large, these numbers fluctuate nearly exactly in phase and therefore the total charge exhibits only small variations ($\pm 0.7e$) around zero. One is tempted to interpret the above observation as evidence for formation of neutral Bjerrum (coion-counterion) pairs [20] inside the pore, and indeed, such pairs and even longer stringlike aggregates of alternating coions and counterions are clearly observable in snapshots of the instantaneous distribution of ions in the pore.

The time histograms of a pore with DNA inside are presented in Fig. 1(b). The time averaged results for the numbers of counterions, coions, and of DNA charges in the pore are summarized in Table I. In the physical case, $\varepsilon_m = 2$, inspection of Table I and Fig. 2(a) reveals that while the counterion concentration in the pore reaches nearly 3 times its value in the bulk, coions are nearly completely depleted from it. The number of counterions appears to be determined by the requirement that the negative charges of the DNA are fully neutralized. Similar counterion enrichment and somewhat smaller coion depletion are observed for abasic DNA (with bases removed) which has a smaller excluded volume but the same charge as normal ssDNA.

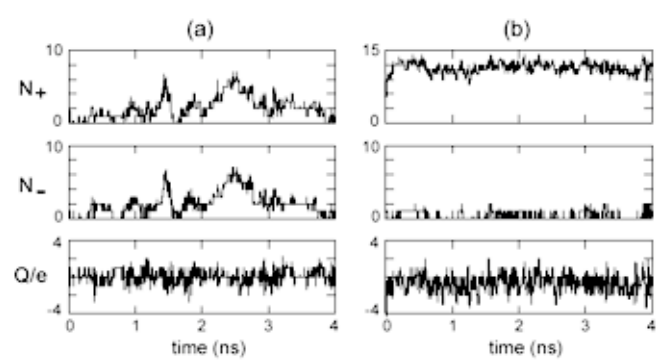

FIG. 1. (a) The time history of the numbers of counterions (N_+), coions (N_-), and the total charges [$Q = e(N_+ - N_-)$] contained in the empty pore (no DNA) is shown. (b) The time history in the presence of DNA (with $N_-^{\mathrm{DNA}} \approx 12$) in the pore. The total instantaneous charge in the pore is $Q = e(N_+ - N_- - N_-^{\mathrm{DNA}})$. In both cases $\varepsilon_m = 2$.

In order to elucidate the role of membrane electrostatics on the distribution of ions in the pore, we increased the dielectric constant of the membrane to its value in water, $\varepsilon_m = 80$. While a fourfold increase in the concentration of coions in the pore compared to the $\varepsilon_m = 2$ case is observed, the number of counterions is nearly unchanged [see Table I and Fig. 2(b)]. We conclude that while the effect of increased electrostatic self-energy of charges surrounded by low dielectric constant medium plays a major role in coion depletion, the number of counterions in the pore is determined mainly by the condition of electroneutrality. This leaves open the question of whether the counterions are condensed (i.e., strongly localized) on the DNA or free to move around the pore. While it is difficult to distinguish between condensed and uncondensed counterions in a narrow pore, inspection of Figs. 2(a) and 2(b) suggests that counterions are more strongly localized on the DNA charges in the low ε_m case. In order to make a quantitative comparison we calculated the appropriate radial distribution functions and found that the probability to find a counterion within 4 Å from a DNA charge is nearly 2 times higher in the $\varepsilon_m = 2$ than in the $\varepsilon_m = 80$ case. This is consistent with the notion that counterion condensation on DNA is more pronounced in the former case, because of the larger electrostatic self-energy of DNA in the pore [19] and with recent theoretical predictions that suggest that condensation in bulk solutions of flexible polyelectrolytes increases with increasing Coulomb strength [21]. Since stronger DNA-counterion coupling should lead to the stiffening of the macromolecule as the result of its ''dressing'' by the counterions, one expects the persistence length of DNA to increase with decreasing ε_m. Indeed, we find that the end-to-end distance is larger and that transverse fluctuations are smaller when $\varepsilon_m = 2$ than when $\varepsilon_m = 80$ (44 Å versus 42 Å, respectively). Further evidence for the renormalization of persistence length scenario comes from comparing the end-to-end distances of abasic, uncharged (with charges removed from spheres representing the phosphate groups), and normal ssDNA. As bases are added to the charged backbone, R increases from 35 to 44 Å and when charges are removed from the latter, R decreases from 44 to 40 Å, in accord with the expectation that the addition of the bulky bases has a larger effect on the persistence length of DNA than its dressing by the small counterions. Since nearly complete coion depletion from the pore is observed only when both (a) DNA is present and (b) $\varepsilon_m = 2$, it must be due to a combination of excluded volume and electrostatic effects. A tentative explanation is that while in the empty pore case Cl^- ions can enter the pore by forming Bjerrum pairs with K^+ ions, such bulky ion pairs are effectively excluded from the pore in the presence of DNA. Since a similar mechanism should apply even if the pore is occupied by a neutral macromolecule, we ran the simulation with uncharged DNA. We find that there are about 1.4 ± 1.0 coions (and the same number of counterions) in the pore, a number intermediate between that corresponding to the empty channel (2.2) and the pore with a charged macromolecule (0.4) cases. This result is consistent with the observations of Ref. [22] on the blockage of α-hemolysin pores by neutral polyethylene glycol polymers, and with the expectation that the charged DNA is ''dressed'' by the neutralizing counterions which increase its excluded volume.

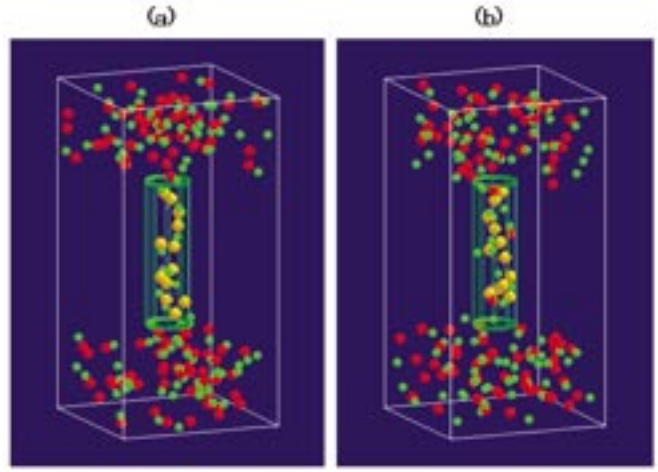

FIG. 2 (color). Snapshot of the ion distribution with ssDNA in the pore for $\varepsilon_m = 2$ (a) and $\varepsilon_m = 80$ (b). Green and red spheres are counterions and coions, respectively, and orange spheres represent the charged phosphate groups of DNA (the neutral sugars and bases are not shown).

In summary, when ssDNA is present in the pore, it is neutralized by counterion condensation; coions, on the other hand, are expelled from the channel. These conclusions remain valid ($N_+ = 13$, $N_- = 1.5$, $N_-^{\mathrm{DNA}} = 12$, $R = 39$ Å) even if we increase the pore radius to 10 Å, a value that is closer to the mean radius of an α-hemolysin channel. In spite of the various assumptions inherent in the present simulation (treating the solution and the membrane as dielectric continua, neglecting hydration, using a simplified model for DNA, and taking no account of the detailed molecular structure of the pore wall), the emerging physical picture of nearly complete counterion condensation and coion depletion in the pore appears to be quite reasonable. Analogy with electrophoresis suggests that the condensed counterions (a) reduce the effective charge of DNA and (b) move together with it in an electric field [23,24]. If this analogy is correct, one is tempted to conclude that these counterions do not take part in charge transport across the pore and that the experimentally observed drop of the ion current in the presence of DNA [4] should be attributed to the reduction in the number of charge carriers due to DNA-induced depletion of coions. However, since the identity of the charge carriers is sensitive to molecular details of the pore neglected in our work (see, e.g., Ref. [18]), the tentative conclusion that residual

conduction through the DNA-blocked pore is due to the negatively charged coions should be tested experimentally, e.g., by changing the chemical composition of the salt molecules.

Stimulating conversations with A. Meller, A. Grosberg, and B. Shklovskii are gratefully acknowledged. Y. R.'s work was supported by a grant from the Israel Science Foundation and supported in part by IMA with funds provided by the NSF. M. T.'s work and travel were supported by Grant-in-Aid No. 16032217 from the Ministry of Education, Science and Culture of Japan. The present computations were performed using supercomputers of the Minnesota University Supercomputing Institute and the Institute of Molecular Science, Japan.

[1] J. Kasianowicz, E. Brandin, D. Branton, and D. Deamer, Proc. Natl. Acad. Sci. U.S.A. **93**, 13770 (1996).
[2] M. Akeson, D. Branton, J. Kasianowicz, E. Brandin, and D. Deamer, Biophys. J. **77**, 3227 (1999).
[3] A. Meller, L. Nivon, E. Brandin, J. Golovchenko, and D. Branton, Proc. Natl. Acad. Sci. U.S.A. **97**, 1079 (2000).
[4] A. Meller, L. Nivon, and D. Branton, Phys. Rev. Lett. **86**, 3435 (2001).
[5] L. Movileanu and H. Bayley, Proc. Natl. Acad. Sci. U.S.A. **98**, 10137 (2001).
[6] D. K. Lubensky and D. R. Nelson, Biophys. J. **77**, 1824 (1999).
[7] E. Slonkina and A. B. Kolomeisky, J. Chem. Phys. **118**, 7112 (2003).
[8] H. Yoon and J. M. Deutsch, J. Chem. Phys. **102**, 9090 (1995).
[9] W. Sung and P. J. Park, Phys. Rev. Lett. **77**, 783 (1996).
[10] N. Lee and S. Obukhov, J. Phys. II (France) **6**, 195 (1996).
[11] E. A. DiMarzio and A. J. Mandell, J. Chem. Phys. **107**, 5510 (1997).
[12] P.-G. de Gennes, Adv. Polym. Sci. **138**, 91 (1999).
[13] M. Muthukumar, J. Chem. Phys. **111**, 10371 (1999).
[14] J. Chuang, Y. Kantor, and M. Kardar, Phys. Rev. E **65**, 011802 (2002).
[15] R. M. Jendrejack, E. T. Dimalanta, D. C. Schwartz, M. D. Graham, and J. J. de Pablo, Phys. Rev. Lett. **91**, 038102 (2003).
[16] A. F. Sauer-Budge, J. A. Nyamwanda, D. K. Lubensky, and D. Branton, Phys. Rev. Lett. **90**, 238101 (2003).
[17] J. Mathé, H. Visram, V. Viasnoff, Y. Rabin, and A. Meller, Biophys. J. **87**, 3205 (2004).
[18] Such effects were taken into account in Brownian dynamics studies of ion permeation through α-hemolysin channel: S. Yu. Noskov, W. Im, and B. Roux, Biophys. J. **87**, 2299 (2004).
[19] A. Parsegian, Nature (London) **221**, 844 (1969).
[20] R. H. Fowler and E. A. Guggenheim, *Statistical Thermodynamics* (Cambridge University Press, Cambridge, England, 1939).
[21] M. Muthukumar, J. Chem. Phys. **120**, 9343 (2004).
[22] L. Movileanu, S. Cheley, and H. Bayley, Biophys. J. **85**, 897 (2003).
[23] C. L. Ma and V. A. Bloomfield, Biopolymers **35**, 211 (1995).
[24] M. Tanaka and A. Grosberg, Europhys. J. E **7**, 371 (2002).